ESTIMATION OF BRAIN RESPONSES BASED ON INDEPENDENT COMPONENT ANALYSIS AND WAVELET DENOISING[1]

Darshan Iyer and George Zouridakis

Biomedical Imaging Lab
Department of Computer Science
University of Houston
Houston, TX, 77204, USA
http://www.cs.uh.edu

Technical Report Number UH-CS-05-01

January 23, 2005

Abstract

Analysis of brain responses on a single-trial basis allows the study of the dynamical characteristics of brain activation. However, single-trial responses are buried into the more prominent background activity, and thus advanced procedures are needed to obtain only the activity of the cortical generators that are activated by the experimental task under study. In this paper, we use simulated data and actual recordings from normal subjects to compare the effectiveness of two methods at removing extraneous activity from single-trial responses, namely, wavelet denoising and our recently proposed procedure, which is based on independent component analysis. Our results show that the new technique can separate individual components from the entire response waveform, and it can also uncover the dynamic evolution of brain responses that cannot be revealed by standard averaging techniques.

ESTIMATION OF BRAIN RESPONSES BASED ON INDEPENDENT COMPONENT ANALYSIS AND WAVELET DENOISING[1]

Darshan Iyer and George Zouridakis

Abstract

Analysis of brain responses on a single-trial basis allows the study of the dynamical characteristics of brain activation. However, single-trial responses are buried into the more prominent background activity, and thus advanced procedures are needed to obtain only the activity of the cortical generators that are activated by the experimental task under study. In this paper, we use simulated data and actual recordings from normal subjects to compare the effectiveness of two methods at removing extraneous activity from single-trial responses, namely, wavelet denoising and our recently proposed procedure, which is based on independent component analysis. Our results show that the new technique can separate individual components from the entire response waveform, and it can also uncover the dynamic evolution of brain responses that cannot be revealed by standard averaging techniques.

Index Terms

Independent Component Analysis, Wavelet Denoising, Brain Activity Analysis, Evoked Potentials.

I. INTRODUCTION

The spontaneous activity of the brain recorded at the scalp as the electroencephalogram (EEG) is of considerably higher amplitude than the activity resulting from external sensory stimulation. The latter, known as evoked potentials (EPs), is typically obtained by averaging a large number of single-trial responses since individual components are typically not visible in single trials. However, single-trial analysis would afford the study of changes in response amplitude, latency, and phase characteristics from trial to trial, and thus, would be better suited than ensemble averaging to study the dynamics of brain activation.

In addition to neural activity, scalp recordings often contain activity from blinks, eye movements, muscle and cardiac activity, interference from power lines, as well as background activity unrelated to the experimental task under study. Ideally, one would like to remove all these "noise" processes and record only the activity of the cortical generators activated by the experimental task, which is the useful "signal".

Early attempts at estimating EPs used Fourier-based filtering techniques [1;2], which, however, were not well suited to the nonstationary nature of the signals. Thus time-adaptive filters were introduced [3; 4] which allowed better adjustment to EP characteristics. Wavelets, which follow the same concept but, in addition, they employ signal-adapted basis functions, have been extensively used to analyze EEG, average EPs [5; 6; 7; 8; 9; 10; 11; 12; 13] and, recently, single-trial EPs [14]. Another technique that was based on a combination of Woody filtering [15] for latency correction in the time domain and wavelet denoising has been proposed to enhance single-trial EPs [16]. This method, however, was shown to work mostly with high-amplitude EPs, while its performance deteriorated for low signal-to-noise ratios (SNRs)

Most of the aforementioned techniques attempt to improve the entire waveform of an average EP. We have recently proposed an alternative methodology [17] for single-trial EP analysis. The technique focuses only on a particular EP component at a time that is made visible on each single trial. Our method is based on independent component analysis (ICA) and the idea that activity resulting from an experimental stimulus is independent from neurophysiological artifacts and background brain activity [18; 19; 20]. The advantage of the method is twofold: it can extract individual components out of the entire average EP waveform, and it can also also provide clear estimates of these components in each single trial. Thus, the method allows studying the dynamic evolution of the underlying cortical generators that give rise to specific EP components. The method has recently been applied to

---

2

obtain EEG and MEG phase maps [21], to classify normal and schizophrenia subjects [22], and improve source localization [23].

In this paper, we compare our ICA-based method for estimating single trial EPs with other techniques, namely, wavelet denoising and plain averaging. For the comparison, we chose the auditory N100 component since, over the past several decades, a plethora of studies, including ours [20; 24; 25], have focused on this EP component recorded from normal subjects [25; 26] and clinical populations [27; 28; 29; 30; 31; 32; 33].

II. METHODS

A. Iterative ICA

Independent component analysis [34] is a method for solving the blind source separation problem [35] which tries to recover N independent source signals, $\mathbf{s} = \{s_1,\ldots,s_N\}$, from N observations, $\mathbf{x} = \{x_1,\ldots,x_N\}$, that represent linear mixtures of the independent source signals. The key assumption used to separate sources from mixtures is that the sources are statistically independent, while the mixtures are not. Mathematically, the problem is described as $\mathbf{x} = \mathbf{As}$, where $\mathbf{A}$ is an unknown mixing matrix, and the task is to recover a version, $\mathbf{u}$, of the original sources, similar to $\mathbf{s}$, by estimating a matrix, $\mathbf{W}$, which inverts the mixing process, i.e., $\mathbf{u} = \mathbf{Wx}$. The estimates $\mathbf{u}$ are called independent components (ICs). The extended infomax algorithm is currently the most efficient technique to solve this problem and relies on a neural network approach and information theory [36; 37; 38; 39].

Our technique, termed iterative ICA (iICA), is an iterative implementation of this algorithm and is applied to a set of recordings consisting of L single trials obtained from N recording channels. Before processing, all single trials are bandpass filtered between 1 and 20 Hz. The procedure is separately applied to all single trials obtained from a particular channel in the following steps:

1. Compute an average EP from all trials.
2. ICA-transform all single trials, grouped in blocks of 10.
3. Compute the absolute correlation values between the current average EP and ICs in all blocks, within a predefined window W_r.
4. Zero those ICs with correlation less than a predefined threshold r_{th}.
5. Inverse-transform the updated ICs back to the time domain, separately in each block.
6. Shuffle the updated single trials around the entire set.
7. Repeat steps 1 to 6 until a convergence criterion is met (see Eq. (5)).

The same procedure is applied to the rest of the channels until all of them have been processed. The parameter values used in the study were $W_r = 50$–250 ms poststimulus, which was consistent with occurrence of the N100-P200 complex, and $r_{th} = 0.15$.

To quantify the improvement in the EP estimate after processing we used two measures, namely the noise reduction factor (NRF) and the mean cross-correlation coefficient (r_{mean}) [16]. The NRF is defined as the ratio between the average RMSE across all trials before and after processing of the data, as shown in Eq. (1).

$$NRF = \frac{^{\mu}RMSE_{original}}{^{\mu}RMSE_{corrected}} \qquad (1)$$

with

$$\mu_{RMSE_X} = \frac{1}{L} \sum_{j=1}^{L} \sqrt{\frac{\sum_{i=1}^{N} (X_{j,i} - EP_i)^2}{\sum_{i=1}^{N} EP_i^2}} \qquad (2)$$

where i refers to time samples, j refers to trials, and EP refers to simulated EP for synthetic data and current template for actual data. A value of *NRF* greater than one indicates improvement after processing; a value of one indicates no improvement; and a value less than one indicates deterioration.

To obtain r_{mean}, the normalized Pearson cross-correlation coefficient is computed between each single trial and the average EP and then the coefficient values are averaged across all single trials, as shown in Eq. (3). The *NRF* is based on estimating the root-mean-squared-error (*RMSE*) between a single trial and the average EP.

$$r_{mean} = \frac{1}{L} \sum_{j=1}^{L} r_{XEP} \qquad (3)$$

where

$$r_{XEP} = \frac{\frac{1}{N} \sum_{i=1}^{N} [(X_i - \mu_X)(EP_i - \mu_{EP})]}{\sigma_X \sigma_{EP}} \qquad (4)$$

r_{mean} : mean cross-correlation coefficient
r_{XEP} : normalized Pearson cross-correlation coefficient between X and EP
σ: standard deviation

The algorithm converged when the absolute difference between successive iterations resulted in NRF value changes of less than 10^{-3}.

B. Wavelet transform (WT)

The WT gives a time-frequency representation of a signal and has an optimal resolution both in the time and the frequency domains. Moreover, WT does not require stationarity of the analyzed signals. The idea behind wavelet analysis is simple: contracted versions of the wavelet function match the high frequency components of the original signal, while dilated versions match low frequency components. Thus, by correlating the original signal with wavelets of different sizes we can obtain its details at different scales. These correlations with the different wavelet functions can be arranged in a hierarchical scheme, called multiresolution decomposition, which separates the signal into 'details' at different scales, while the remaining part is a coarser representation of the signal, called an 'approximation'.

In this study, quadratic bi-orthogonal B-Splines [40] were chosen as the basic wavelet, due to their similarity with the component EP, which would give good localization in the wavelet domain [12; 14; 40; 41; 42]. Furthermore, we used a 7-level decomposition, thus having 7 scales of details (d_1–d_7) and a final approximation (a_7). The lower levels give the details corresponding to high frequency components and the higher levels the ones corresponding to low frequencies.

For WT-based denoising, the basic assumption is that the WT separates the signal and the noise-related components into different scales. For each trial, a wavelet transform W is computed. Let μ denote the mean of the wavelet coefficients calculated over all L single trials, and σ^2 the corresponding variance. Then, we can expect the ratio μ^2/σ^2 to be higher in signal than in noise related coefficients if EPs are similar across trials. The thresholding scheme used in this paper [16] is given as

$$w_j^* = \begin{cases} w_j, & \text{if } |\mu_j| \geq \dfrac{2\sigma_j}{\sqrt{L}} \\ 0, & \text{otherwise} \end{cases} \tag{5}$$

Thus, the inverse WT of w_j^* would lead to denoised EPs in the time domain.

C. Data

In our analysis, we used both synthetic data and actual data obtained at two different labs.

Synthetic data

A simulated EP (true signal) of length 700 ms was generated by adding two half-wave sinusoids with frequency 8.25 Hz and 6.25 Hz, respectively, and peak-to-peak amplitude of 12 μV, simulating a biphasic N100-P200 complex. To obtain synthetic single trial responses, the simulated EP was added to actual background EEG segments, each of length 700 ms, in the time range consistent with the occurrence of N100-P200 complex at different delays (d) which could vary between 0 and 25 ms. Several synthetic sets were generated by changing the signal-to-noise ratio (SNR) which was allowed to vary between 0.2 and 1, and was defined as [25],

$$SNR = \frac{1}{L} \sum_{i=1}^{L} \frac{\sigma_{EP}^2}{\sigma_{EEG_i}^2} \tag{6}$$

where L is the number of single trials, σ_{EP}^2 the variance of the simulated EP, and $\sigma_{EEG_i}^2$ the variance of the ith EEG segment.
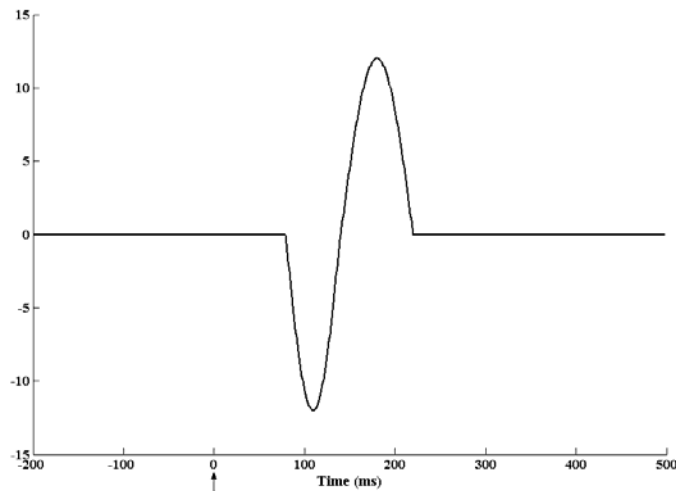

Fig. 1. True EP. Artificial signal simulating the N100-P200 complex of an evoked response.

Real Data

To test the generality of the methods, the data analyzed in this study were produced at two different labs, namely the Biomedical Imaging Lab at the University of Houston (UH) and the Department of Psychiatry at Yale University School of Medicine (Yale). All subjects were volunteers and gave written informed consent to the studies.

Dataset 1

Recordings were made at UH in a quiet but not electrically shielded room, using a 256-channel, active electrode, dense-array EEG recording system (model ActiveTwo, BioSemi Biomedical Instrumentation, The Netherlands). Stimuli consisted of tones of 1 kHz delivered binaurally at a rate of 1.1 stimuli per second. A total of 200 trials were collected in each recording session, but subsequent removal of artifacts, e.g., eye blinks, eye movement, muscle activity, with absolute amplitude greater than 75 µV, resulted in each set having between 150 and 200 trials.

Dataset 2

Recordings were made at Yale in a quiet but not electrically shielded room, using nine channels of a Neuroscan EEG recording system. Stimuli consisted tones of 1 kHz tones delivered binaurally at the rate of one stimulus every 8 s. Initially, a total of 100 trials were collected in each recording session but subsequent removal of artifacts, e.g., eye blinks, eye movement, muscle activity, with absolute amplitude greater than 75 µV, resulted in each set having between 45 and 100 trials.

Data from both sets were digitized at sampling rate of 1 kHz per channel and stored on the hard disk for off-line analysis. Data were segmented into 700 ms epochs, each containing 200 ms prestimulus and 500 ms poststimulus activity before further processing. Data from only the Cz channel were used for the analysis.

The performance of WT denoising and *i*ICA procedures was tested with synthetic data under different d and SNR conditions. Statistical analysis was done using t tests for the sample mean.

III. RESULTS

A. Synthetic data

We generated 200 synthetic single trials using SNR = 0.2 and d = 0-25 as explained earlier and the WT-based and ICA-based methods were applied to the data. Figure 2 depicts the results of denoising action on single trials (Synthetic: left, wavelet: middle and iterative ICA: right.). Figure 3 shows the true EP signal and the estimates obtained after plain averaging (EP$_{ave}$), WT-based denoising (EP$_{wave}$), and ICA-based denoising (EP$_{ICA}$). It took around thirty-five iterations for the *i*ICA algorithm to converge. Both procedures were fast.
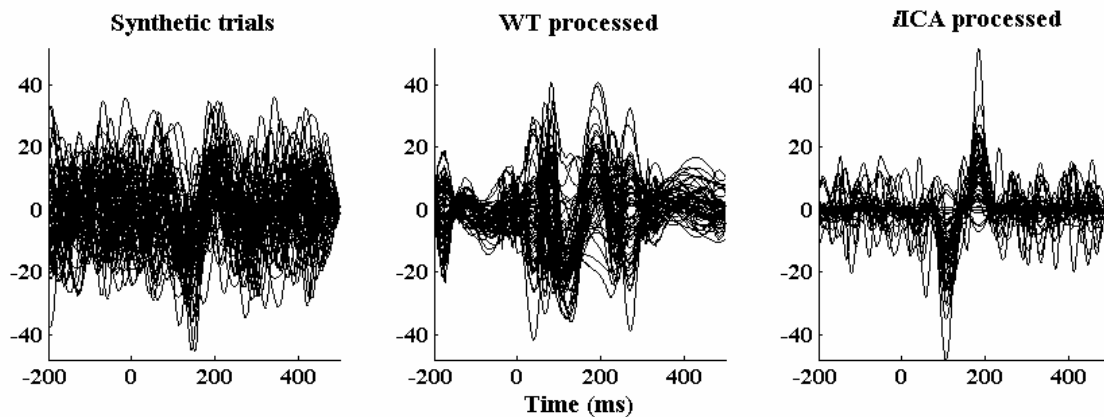

Fig. 2. Denoising on single trials. Original single-trial responses (left) and the resulting denoised ones after WT (middle) and *i*ICA processing.
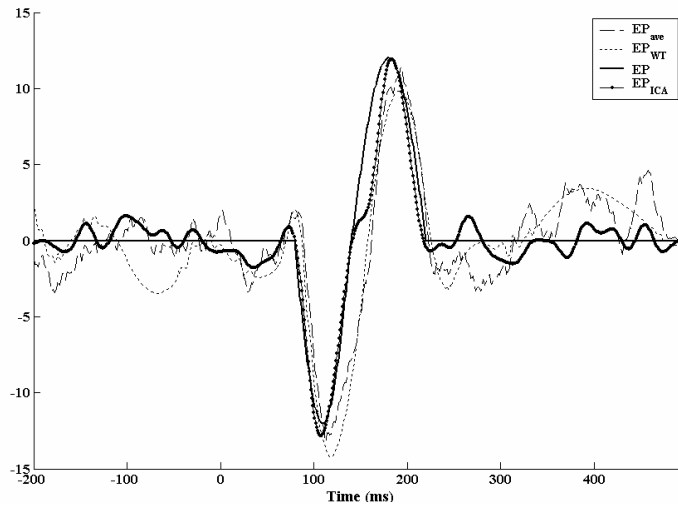
Fig. 3. Denoising on ensemble average responses. True EP signal (solid) and estimates obtained using plain averaging EP_{ave} (dashed), WT-based denoising EP_{WT} (dotted), and ICA-based denoising EP_{ICA} (dot-dashed). SNR = 0.2 and d = 0-25 ms.

Effect of SNR at different delays

The ability of the methods to estimate an EP was studied using different delays, which varied from 5 to 25 ms in increments of 5 ms, and SNR, which varied between 1.0 and 0.2 in decrements of 0.2. For each combination, the algorithm was executed twenty times and at the end of each run the *NRF* and r_{mean} was computed.

Figure 4 shows the *NRF* values obtained for the WT and *i*ICA methods. The values plotted are the means and the standard errors across twenty runs. Both methods gave NRF values significantly greater than one (p < 0.01) indicating that the RMSE decreased after processing and that the resulting EP improved. Although the WT and *i*ICA procedure had similar performance, the ICA procedure gave significantly greater *NRF* values ($p < 0.01$) for each combination of SNR and *d* as revealed by separate t-tests.

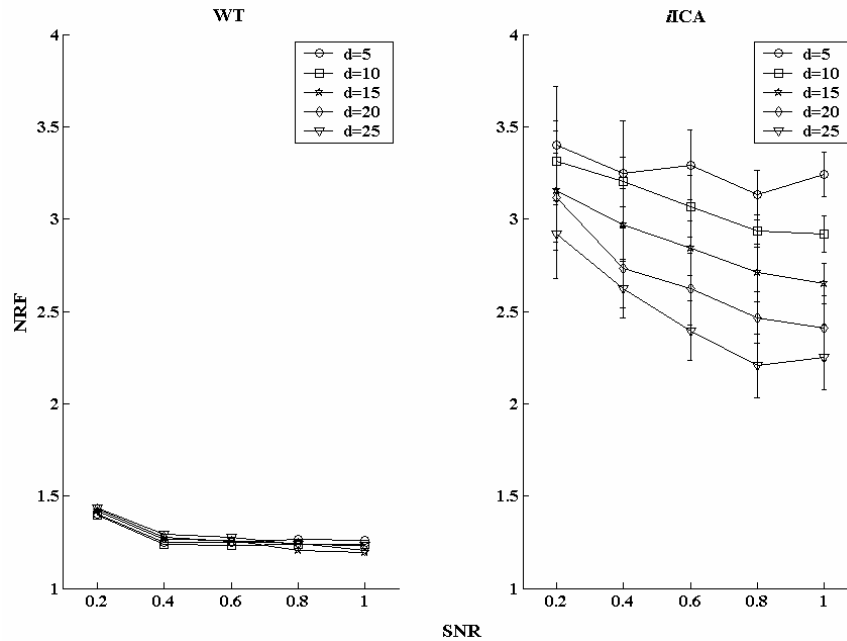
Fig. 4. Effect of SNR at different delays in terms of NRF. NRF at different d and SNR for WT (left) and iICA (right) denoising.

Figure 5 depicts the performance of WT and *i*ICA in terms of r_{mean} defined earlier. The left panel shows the r_{mean} values for the synthetic trials before the processing. Each trial contains the true EP but due to noise contamination,

7

the correlation between the true EP and the trials is low (0.35 to 0.65). However, after processing, the r_{mean} increases as shown in the middle (Wavelet: 0.5 to 0.8) and the right panels (Iterative ICA: 0.73 to 0.98). Although the WT denoising follows a similar performance trend as the iICA procedure, the later gave significantly greater r_{mean} values ($p < 0.01$) for all SNR and d conditions.
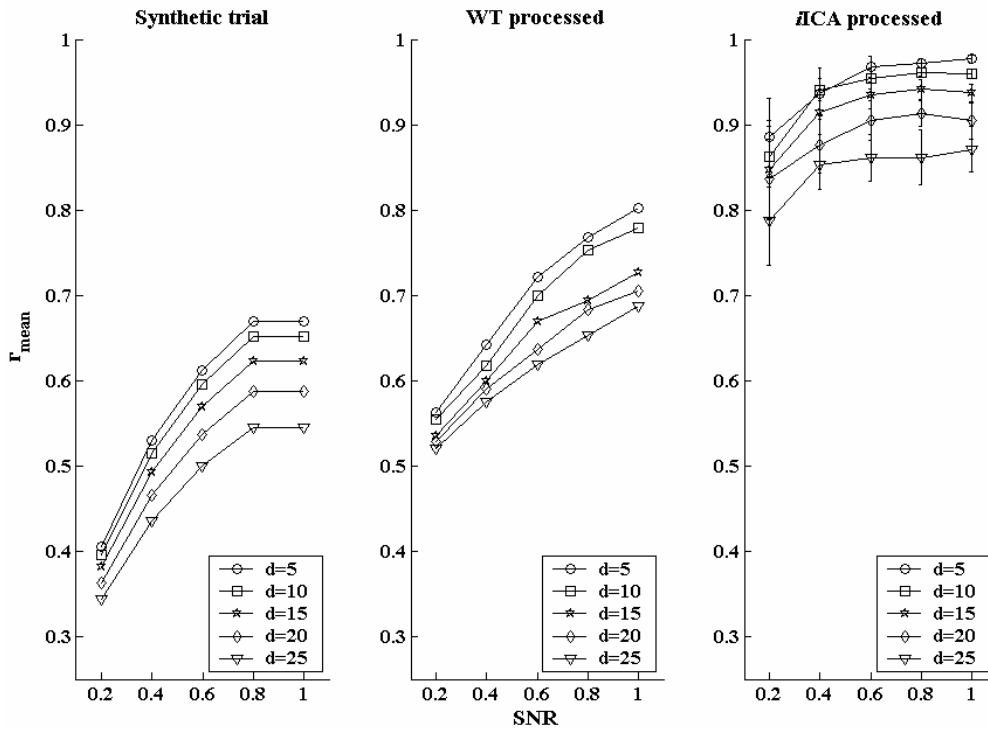

Fig. 5. Effect of SNR at different delays in terms of r_{mean}. r_{mean} at different d and SNR for WT (left) and iICA (right) denoising.

B. Results with actual data

Figures 6 shows example of the performance of the WT and iICA procedures on actual data (two subjects from dataset 2). The top panels show the single trials and the corresponding averages are shown in the bottom panels. Figure 6a shows a typical subject whereas Figure 6b shows a noisy subject.
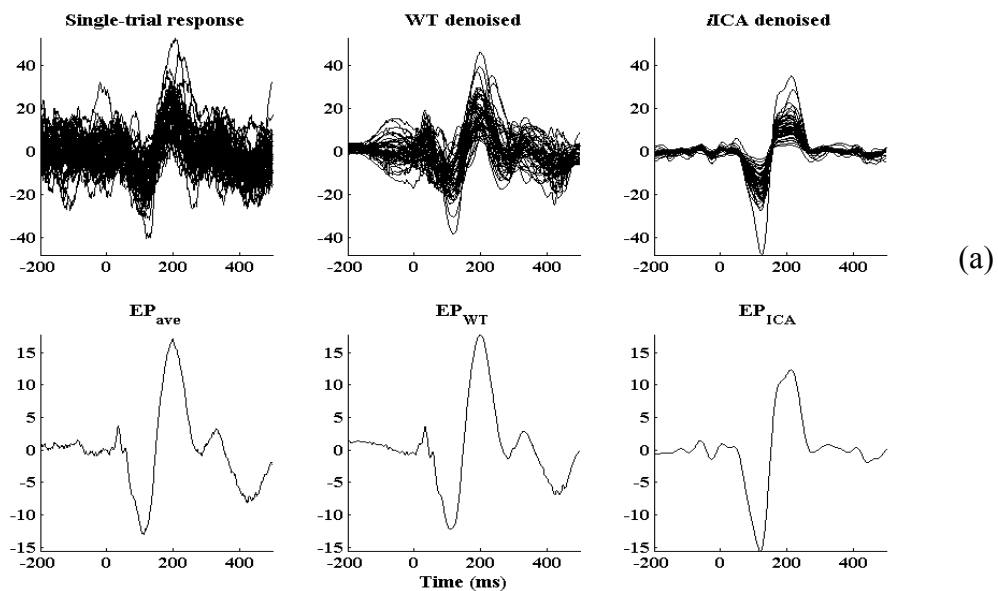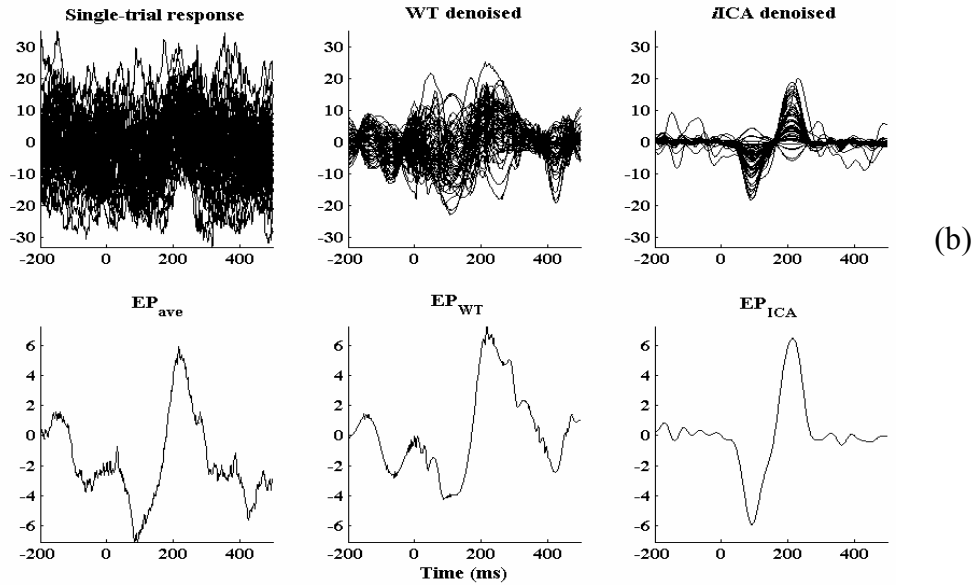
Fig. 6. Denoising on dataset 2. Original single-trial responses (left) and the resulting denoised ones after WT and *i*ICA (right) processing. The corresponding averages are shown in the bottom panels.

Figures 7 shows example of the performance of the WT and *i*ICA procedures on actual data (two subjects from dataset 1). The top panels show the single trials and the corresponding averages are shown in the bottom panels. Figure 7a shows a typical subject whereas Figure 7b shows a noisy subject.
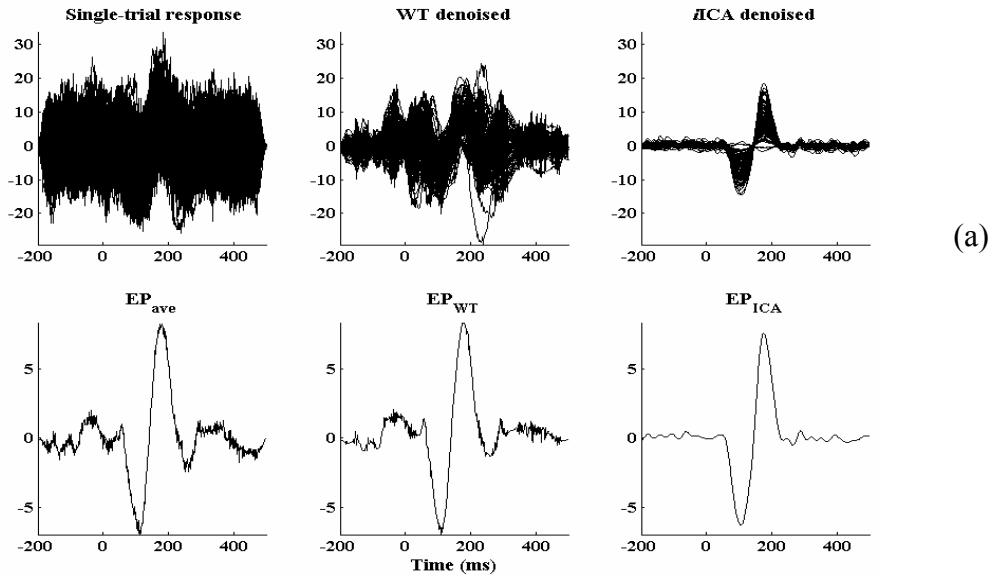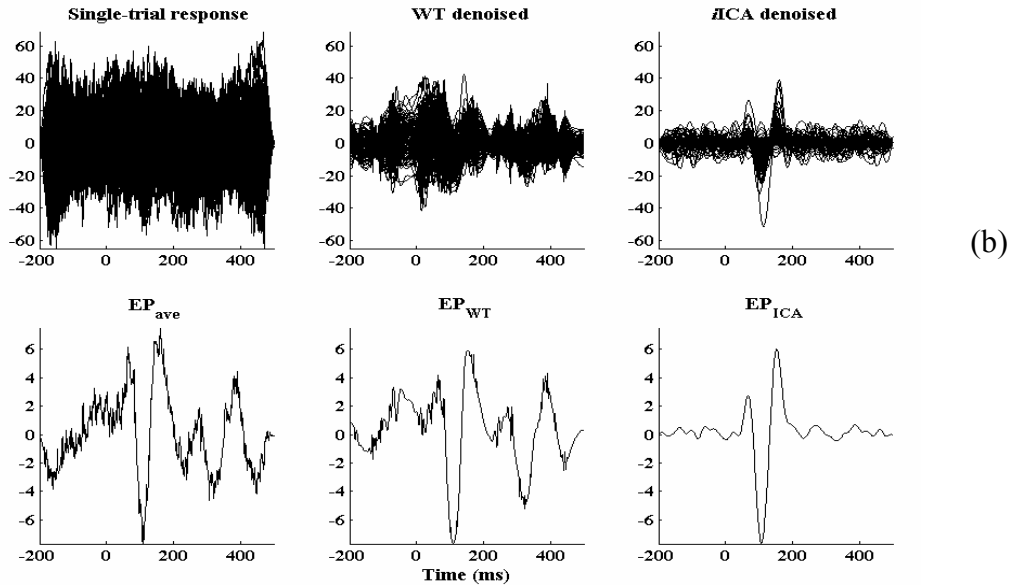
Fig. 7. Denoising on dataset 1. Original single-trial responses (left) and the resulting denoised ones after WT and *i*ICA (right) processing. The corresponding averages are shown in the bottom panels.

IV. DISCUSSION

The usual way to visualize the EPs is by means of ensemble averaging due to SNR issues. However, when averaging, information about the single trial variability is lost.

In this paper, *i*ICA method was compared to WT-based denoising and classical averaging using simulated and actual auditory EPs. The focus was to study the applicability of the methods to extract single trial N100-P200 responses.

With simulated data, the *i*ICA approach provided significantly better estimates of the true EP compared to plain averaging ($p < 0.01$) and WT-based denoising ($p < 0.01$). Even in the worst experimental conditions (SNR = 0.2 and d = 0-25 ms), the latency of the N100 peak estimated using *i*ICA was closer to that of the true EP. From a single trial perspective, the *i*ICA gave statistically greater *NRF* and r_{mean} values under all experimental conditions ($p < 0.01$). In general, differences between the plain averaged EPs and *i*ICA EPs became smaller as the SNR was increasing. This suggests that *i*ICA does not introduce any major artifact in the reconstruction of the EPs. The technique performs well even at very low SNRs (=0.2).

When actual data were used, the iICA procedure showed responses in single trials, which typically are difficult to see due to low SNR. In the corresponding average EPs, the N100-P200 peaks become sharper and the data outside the region of interest become flatter giving an enhanced view of the N100 components. Though we see similar patterns in WT denoised single trials, the peaks are scattered and widely distributed resulting in less clear N100 component in the average EP.

The above results suggest that the *i*ICA technique gives access to dynamic evolution of N100-P200 complex that cannot be revealed by standard averaging techniques. Since the method analyzes one channel at a time, it can be applied to large multi-channel datasets.

We found that the WT denoising gave an apparently smoother overall EP, while *i*ICA could separate individual components from the entire EP waveform, and also provide clear estimates of these components in each single trial.

REFERENCES

[1] Doyle, D. J., "Some comments on the use of Wiener filtering in the estimation of evoked potentials," *Electroenceph Clin Neurophysiol.*, vol. 38 pp. 533-534, 1975.

[2] Walter, D. O., "A posteriori Wiener filtering of average evoked response," *Electroenceph Clin Neurophysiol.*, vol. 27 pp. 61-70, 1969.

[3] De Weerd, J. P., "posteriori time-varying filtering of averaged evoked potentials. I. Introduction and conceptual basis," *Biological Cybernetics*, vol. 41 pp. 211-222, 1981.

[4] De Weerd, J. P. and Kap, J., I, "A posteriori time-varying filtering of averaged evoked potentials. II. Mathematical and computational aspects," *Biological Cybernetics*, vol. 41 pp. 223-234, 1981.

[5] Adeli, H., Zhou, Z., Dadmehr, N., "Analysis of EEG records in an epileptic patient using wavelet transform," J *Neurosci Methods* 123(1), 69-87. 2-15-2003.

[6] Bartnik, E. A. and Blinowska, K. J., "Wavelets-new method of evoked potential analysis," *Med.Biol.Eng.Comput.* , vol. 30 pp. 125-126, 1992.

[7] Bradley, A. P. and Wilson, W. J., "On wavelet analysis of auditory evoked potentials," *Clin Neurophysiol.*, vol. 115 pp. 1114-1128, May2004.

[8] Demiralp, T., Ademoglu, A., Schurmann, M., Basar-Eroglu, C., and Basar, E., "Detection of P300 waves in single trials by the wavelet transform (WT)," *Brain Lang.*, vol. 66 pp. 108-128, Jan.1999.

[9] Jerger, K. K., Netoff, T., I, Francis, J. T., Sauer, T., Pecora, L., Weinstein, S. L., and Schiff, S. J., "Early seizure detection," *J Clin Neurophysiol.*, vol. 18 pp. 259-268, May2001.

[10] Samar, V. J., Bopardikar, A., Rao, R., and Swartz, K., "Wavelet analysis of neuroelectric waveforms: a conceptual tutorial," *Brain Lang.*, vol. 66 pp. 7-60, Jan.1999.

[11] Senhadji, L. and Wendling, F., "Epileptic transient detection: wavelets and time-frequency approaches," *Neurophysiol Clin.*, vol. 32 pp. 175-192, June2002.

[12] Schiff, S. J., Aldrouby, A., Unser, M., and Sato, S., "Fast wavelet transformation of EEG," *Electroenceph Clin Neurophysiol.*, vol. 91 pp. 442-455, 1994.

[13] Zhang, J. and Zheng, C., "Extracting evoked potentials with the singularity detection technique," *IEEE Eng Med Biol Mag.*, vol. 16 pp. 155-161, Oct.1997.

[14] Quiroga, R. Q. and Garcia, H., "Single-trial event-related potentials with wavelet denoising," *Clinical Neurophysiology*, vol. 114 pp. 376-390, 2003.

[15] Woody, C. D., "Characterization of an adaptive filter for the analysis of variable laterncy neuroelectric signals," *Med.Biol.Eng.*, vol. 5 pp. 539-553, 1967.

[16] Effern, A., Lehnertz, K., Grunwald, T., Fernandez, G., David, P., and Elger, C. E., "Time adaptive denoising of single trial even-related potentials in the wavelet domain," *Psychophysiology*, vol. 37 pp. 859-865, 2000.

[17] Zouridakis, G. and Iyer, D., "Improved Estimation of Evoked Potentials Using an Iterative Independent Component Analysis Procedure," *2nd WSEA International Conference on Signal Processing Robotics and Automation Mykonos Greece ISPRA 2003*, Jan.2004.

[18] Vigario, R. N., "Extraction of ocular artifacts from EEG using independent component analysis," *Electroenceph Clin Neurophysiol.*, vol. 103 pp. 395-404, 1997.

[19] Makeig, S., Westerfield, M., Jung, T.-P., Covington, J., Townsend, J., Sejnowski, T. J., and Courchesne, E., "Independent components of the late positive response complex in a visual spatial attention task," *J Neurosci.*, vol. 19 pp. 2665-2680, 1999.

[20] Makeig, S., Westerfield, M., Jung, T. P., Enghoff, S., Townsend, J., Courchesne, E., and Sejnowski, T. J., "Dynamic brain sources of visual evoked responses," *Science*, vol. 295 pp. 690-694, 2002.

[21] Iyer D.and Zouridakis G., "EEG and MEG Phase Maps using Iterative Independent Component Analysis," *22nd Annual Houston Conference on Biomedical Engineering Research* . Feb 2005.

[22] Iyer D.and Zouridakis G., "Single-Trial P50 Analysis Improves Separation of Normal and Schizophrenia Population," *22nd Annual Houston Conference on Biomedical Engineering Research* . Feb 2005.

[23] Iyer D.and Zouridakis G. "Computational improvements in electric source imaging of auditory N100 component," *Keck Center/HAMBP Annual Research Conference* . Oct 2004.

[24] Iyer, D., " Measurement of phase synchronization in auditory evoked potentials" *Master's thesis, University of Houston* . May 2001.

[25] Zouridakis, G., Jansen, B. H., and Boutros, N. N., "A Fuzzy clustering approach to EP estimation," *IEEE Trans.Biomed.Eng.*, vol. 44 pp. 673-680, 1997.

[26] Young, K. A., Smith, M., Rawls, T., Elliott, D. B., Russell, I. S., Hicks, P. B., "N100 evoked potential latency variation and startle in schizophrenia", . *Neuroreport* 12 (4): 767-773. 3-26-2001.

[27] Boutros, N., Nasrallah, H., Leighty, R., Torello, M., Tueting, P., Olson, S., "Auditory evoked potentials, clinical versus research applications", *Psychiatry Res*. 69 (2-3), 183-195. 1997.

[28] Buchsbaum, M. S., "The middle evoked response components and schizophrenia". *Schizophr Bull*. 1, 93-104. 1997.

[29] Clementz, B. A., Geyer, M. A., Braff, D. L. "Poor P50 suppression among schizophrenia patients and their first-degree biological relatives," *Am J Psychiatry*. 155 (12), 1691-1694. 1998.

[30] Ford, J. M., Mathalon D. H., Kalba, S., Marsh, L., Pfefferbaum, A. "N1 and P300 abnormalities in patients with schizophrenia, epilepsy, and epilepsy with schizophrenialike features," *Biol Psychiatry* [1], 848-860. 2001. Ref Type: Generic

[31]   Iyer D.and Zouridakis G. "Single-Trial EP Analysis Improves Separation of Normal and Schizophrenia Subjects", *6th ECNS Annual Conference* . 9-23-2004.

[32]   Straumanis, J. J., "Event-related potentials in schizophrenia", *Psychiatr Med*. 8 (1), 53-72. 1990.

 [33]   Winterer, G., Ziller, M., Dorn, H., Frick, K., Mulert, C., Wuebben, Y., Herrmann, W. M., Coppola, R., "Schizophrenia: reduced signal-to-noise ratio and impaired phase-locking during information processing", *Clin Neurophysiol.*, 111(5): 837-849, May 2000.

[34]   Comon, P., "Independent component analysis—a new concept?," *Signal Proc.*, vol. 36 pp. 287-314, 1994.

[35]   Jutten, C. and Herault, J., "Blind separation of sources I. An adaptive algorithm based on neuromimetic architecture," *Signal Processing*, vol. 24 pp. 1-10, 1991.

[36]   Bell, A. and Sejnowski, T., "An information -maximization approach to blind source separation and blind deconvolution," *Neural Computation*, vol. 6 pp. 1129-1159, 1995.

[37]   Girolami, M., "An alternative perspective on adaptive independent component analysis algorithms," *Neural Computation*, vol. 10 pp. 2103-2114, 1998.

[38]   Jung, T.-P., Makeig, S., Westerfield, M., Townsend, J., Courchesne, E., and Sejnowski, T. J., "Removal of eye activity artifacts from visual event-related potentials in normal and clinical subjects," *Clin Neurophys.*, vol. 111 pp. 1745-1758, 2000.

[39]   Lee, T. W., Girolami, M., and Sejnowski, T. J., "Independent component analysis using an extended infomax algorithm for mixed sub-Gaussian and super-Gaussian sources," *Neural Comput.*, vol. 11 pp. 417-441, 1999.

[40]   Cohen, A., Daubechies, I., and Feauveau, J. C., "Bio-orthogonal bases of compactly supported wavelets," *Comm Pure Appl Math.*, vol. 45 pp. 485-560, 1992.

[41]   Chui, C., "An introduction to wavelets," *San Diego: Academic Press*, 1992.

[42]   Unser, M., "Ten good reasons for using spline wavelets," *Proc.SPIE Wavelets applications in Signal and Image Processing*, vol. 3169 pp. 422-431, 1997.